Bull. Chem. Soc. Ethiop. **2005**, 19(2), 277-288. ISSN 1011-3924
Printed in Ethiopia © 2005 Chemical Society of Ethiopia

SYNTHESIS OF MESOPOROUS TITANIUM OXIDE AND CATALYTIC ACTIVITY OF Ru/m-TiO_2

Xuehong Zhang[1,2], Laitao Luo[1*] and Zhanhui Duan[1]

[1]Institute of Applied Chemistry, Nanchang University, Nanchang 330047, Jiangxi, PR China
[2]Nanchang Institute of Aeronautical Technology, Nanchang 330034, Jiangxi, PR China

(Received November 22, 2004; revised March 1, 2005)

ABSTRACT. A series of mesoporous TiO_2 oxide (m-TiO_2) were synthesized by using n-cetylpyridinium chloride (C_{16}PyCl) as a structure-directing agent under complete different conditions. The synthesized mesoporous samples were characterized by means of FT-IR, XRD, and N_2 adsorption methods. Effects of template, solvent, pH, ageing temperature and C_{16}PyCl/TTIP molar ratio on the structure and stability of m-TiO_2 were also discussed. The results show that the property of m-TiO_2 synthesized by using C_{16}PyCl as template, C_2H_5OH as solvent, pH 7-8, ageing temperature 20 °C and C_{16}PyCl/TTIP molar ratio 2 are superior to that of m-TiO_2 prepared under other conditions. After being loaded by the impregnating method, the Ru particle strongly interacts with the mesoporous supports. The catalytic activity of Ru/m-TiO_2 for methanol decomposition to carbon monoxide and hydrogen was investigated. It is found that synthesizing conditions of mesoporous materials affect the catalytic activity of Ru/m-TiO_2.

KEY WORDS: Mesoporous titanium oxide, Methanol decomposition, Ruthenium, Catalyst support, n-Cetylpyridinium chloride

INTRODUCTION

Mesoporous materials, for example silicic MCM-41, have been often employed as a catalyst support and showed significant catalytic activity, probably because the active metals can be highly dispersed in the characteristic pore structure with high surface area [1]. Titania is attractive for its potential applications, e.g., photocatalysts [2], electrodes for wet solar cells [3], etc. For many applications, porous titania with a large surface area is suitable. The successful synthesis of stable mesoporous TiO_2 involves the application of tetradecylphosphate surfactant as a template and removing it by calcinations [4]. However, the structure is probably destroyed after the removal of the surfactant by a thermal treatment. Antonelli [5] and Dai *et al*. [6] have reported that the best pH condition for the synthesis of mesostructure TiO_2 materials was in the range of 4-6 (using phosphate and long-chain alkylamine surfactant, respectively.), and that changing the pH value brought little effect on the formation of mesostructure. Since thermal stability is usually required as a catalyst support, it is necessary to obtain the thermally stable mesoporous TiO_2 powder. So far, it has not been reported on the synthesis of mesoporous TiO_2 by using n-cetylpyridinium chloride (C_{16}PyCl)) as a template and the effects of synthesizing conditions. For the probe reaction of methanol decomposition to carbon monoxide and hydrogen, new catalysts being active at low temperatures below 200 °C are required [7]. Various metals like nickel, copper, platinum and palladium supported over Al_2O_3, SiO_2, TiO_2, ZrO_2, CeO_2 and synthetic clays are reported to be effective for the methanol decomposition to CO and H_2 [8-13]. But for such reaction system, the research on using Ru as active component and m- TiO_2 as support has not been reported.

*Corresponding author. Tel.: +86 791 8305822. E-mail address: luolaitao@yahoo.com.cn

In this paper, mesoporous TiO_2 powder with high surface area was synthesized by using $C_{16}PyCl$ as a template, and their physicochemical properties were investigated by means of FT-IR, XRD and N_2 adsorption methods. In the mean time, we studied the effects of preparation conditions of m-TiO_2 on the catalytic activities of Ru/m-TiO_2 catalysts in the methanol decomposition.

EXPERIMENTAL

Synthesis of m-TiO_2 material

Mesoporous TiO_2 were synthesized as follows: 4 g different surfactants (n-cetylpyridinium chloride ($C_{16}PyCl$), alkyl polyglycol ether ($(C_2H_4O)_nC_{12}H_{26}O$) or hexadecyltrimethyl ammonium bromide ($C_{16}H_{33}NBr(CH_3)_3$)) was dissolved in 20 mL solvents (ethyl alcohol absolute (C_2H_5OH), n-butanol (C_4H_9OH) or chloroform ($CHCl_3$)), respectively, and 1.94 g tetra-n-butyl titanate (TTIP) was added. The mixture was stirred for 30 min at room temperature and then added 196 g deionized water slowly. This led to a solid precipitate. The pH of the solution was then adjusted with NaOH to 3-4, 7-8 or 9-10, respectively. Mesitylene (MES, 1.96 g) was added into the solution. The resultant solid product in the solution was allowed to stand for 3 days at 20, 40, 60 or 80 ^oC, respectively. The filtered products were additionally treated in a phosphoric acid solution (0.1 M) for about 2 h to enhance the thermal stability of the solid products. The products were dried at 100 ^oC for 3 h. Synthesizing conditions of m-TiO_2 material are summarized in Table 1. Subscript 20, 40, 60, 80 represent the aged temperature 20, 40, 60, 80 ^oC, respectively.

Table 1. The synthesizing conditions of m-TiO_2.

Samples	A_{20}	A_{40}	A_{60}	A_{80}	A(acid)	A(base)	B	C	D	E
Surfactant	$C_{16}PyCl$	$C_{16}PyCl$	$C_{16}PyCl$	$C_{16}PyCl$	$C_{16}PyCl$	$C_{16}PyCl$	$C_{16}PyCl$	$C_{16}PyCl$	$(C_2H_4O)_nC_{12}H_{26}O$	$C_{16}H_{33}NBr(CH_3)_3$
Solvent	C_2H_5OH	C_2H_5OH	C_2H_5OH	C_2H_5OH	C_2H_5OH	C_2H_5OH	C_4H_9OH	$CHCl_3$	C_2H_5OH	C_2H_5OH
Aging temp. (^oC)	20				20	20	20	20	20	20
pH	7-8	7-8	7-8	7-8	3-4	9-10	7-8	7-8	7-8	7-8

Preparation of ruthenium catalysts

A 1% ruthenium was supported on mesoporous TiO_2 using 0.01 M solution of ruthenium chloride by the impregration method. After impregnating for 24 h, the sample was dried at 120 ^oC overnight and calcined in air at 400 ^oC for 2 h.

Catalytic activity measurement

Gas phase methanol decomposition was performed in a pulsed micro-catalytic reactor (stainless steel U-shaped tube, 6 mm inner diameter). The temperature was raised from room temperature up to 400 ^oC with a heating rate of 5 $^oC\ min^{-1}$ controlled by a temperature programmer, the catalyst was reduced in a flow of 10 vol. % hydrogen diluted with nitrogen (flow rate, 10 cm^3min^{-1}) for 2 h at 400 ^oC, and then decreased for 30 min. The weight of catalyst was 0.03 g diluted with 1.0 g of quartz sand for each of the experiments. Each time 1 μL reactant was injected into the reactor. The product was analyzed by gas chromatography equipped with a Porapark-Q column (2 m) and a thermal conductivity detector, connected with a computer

integrator system. The temperature of the column is 60 ^oC. The catalytic activity is assigned as hydrogen selectivity.

Characterization

Powder X-ray diffraction (XRD) patterns of the samples were recorded with D8 ADVNCE (Brucker company in Germany) diffractometer using nickel-filtered CuKα radiation. The diffractometer was operated at 40 kV and 30 mA of tube voltage and current, respectively. The mesopore size distribution was determined from the desorption isotherm of nitrogen obtained with ST-2000 (Beijing analytic instrument factory). The BET surface areas and the total pore volume of the samples were also determined. The framework vibration IR spectra of the samples were investigated on a WQF-200 Fourier transform instrument (Beijing second optical instrument factory) with KBr wafer technique. Thermogravimetry-differential thermal analysis (TG-DTA) was recorded by ZRY-2P (Shanghai exact scientific instrument corporation) instrument in air atmosphere with 10 ^oC min^{-1}.

RESULTS AND DISCUSSION

Ti-skeleton of mesoporous TiO_2 (m-TiO_2) framework

The FT-IR spectra of m-TiO_2 (A_{20}) calcinated at different temperature are shown in Figure 1. The IR band at about 3300-3500 cm^{-1} and 1600 cm^{-1} is usually taken as vibration spectrum of O-H in water, the band of 2800-2900 cm^{-1} is corresponding to the vibration spectrum of C-H in alkyl chain. It shows that surfactants are intercalated into hydrous titanium oxide. The band of 960 cm^{-1} belongs to the vibration spectrum of Ti-O in TiO_2 crystal. After removal of template by calcinations at 400 ^oC, FT-IR spectra of m-TiO_2 are similar to that of Ti-MCM-41 [14]. The disappearance of vibration spectrum at 2800-2900 cm^{-1} indicate that surfactants intercalated hydrous titanium oxide have been already removed completely. The new band at about 2300 cm^{-1} may be due to lattice defects induced by high temperature treatment [15]. The IR band at about 960 cm^{-1} is usually taken as evidence at the relevant concentration of Ti-skeleton [14]. The intensity of this band increases with the increase in Ti content of m-TiO_2, which indicates that all the Ti of m-TiO_2 may be incorporated into the channel wall.

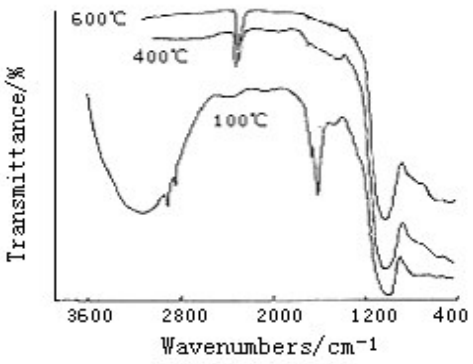

Figure 1. FT-IR spectrum of m-TiO_2(A_{20}) calcinated at different temperature.

Study on the synthesis conditions

A series of experiments were carried out to find better conditions for synthesizing mesoporous TiO_2. The pH value of precursor solutions, ageing temperature, the molar ratio of $C_{16}PyCl$, the variation of templates and solvents were mainly adjusted. The pH value was varied in the range of 3-10, the ageing temperature were adjusted in the region of 20-80 ^oC, the molar ratio of $C_{16}PyCl$ to TTIP ratio was studied at 0.5-3, the templates were $C_{16}PyCl$, $(C_2H_4O)_nC_{12}H_{26}O$ and $C_{16}H_{33}NBr(CH_3)_3$, respectively, the solvents were C_2H_5OH, C_4H_9OH and $CHCl_3$, respectively. In all cases, while one parameter was changed, the others were held constant.

Effect of variation of templates

In order to determine the ideal surfactant as template for the synthesis of m-TiO_2, a few surfactants had been tried as the template in our experiments. Figure 2 shows the XRD patterns of samples A_{20}, D and E, whose templates are $C_{16}PyCl$, $(C_2H_4O)_nC_{12}H_{26}O$ and $C_{16}H_{33}NBr(CH_3)_3$„ respectively. As shown in Figure 2, as-synthesized m-TiO_2 exhibit low angle reflections of mesoporous materials [16]. No peak is observed at $2\theta>10°$, excluding any ordinary crystalline phase of the surfactant or titanium species. Nevertheless, the sample A_{20} shows a more intensive diffraction peak with comparison to D and E, which is attributed to the relatively order mesoporous structure of the channels. It also indicates that the uniformity of D and E are obviously inferior to that of A_{20}. Figure 3 shows the thermogravimetric analysis curves of A_{20}, D and E, which indicates the strong interactions of the associated template with titanium groups. The weight loss at 56-170 ^oC is due to the desorption of water. The weight loss above 170 ^oC is attributed to the combustion of organic compounds; that is to say, this weight reduction is due to the removal of templates. The observed continuous weight loss of A_{20}, D and E are 24.5%, 6% and 15.99%, respectively, this indicates by the fact that the amount of surfactant linked with Ti species is related with the chain length. At the same time, this result also shows that there are the larger amount of surfactant linked with Ti species in A_{20}.

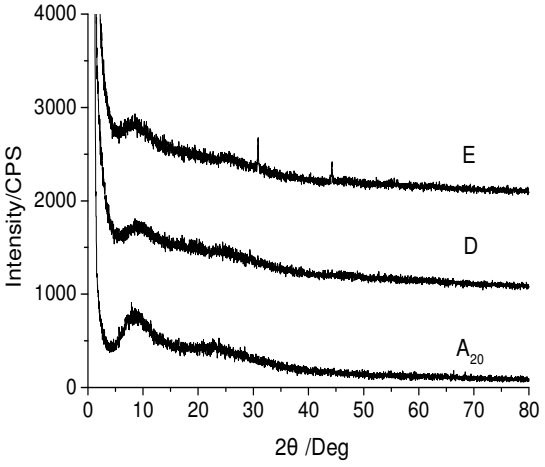

Figure 2. XRD patterns of the samples.

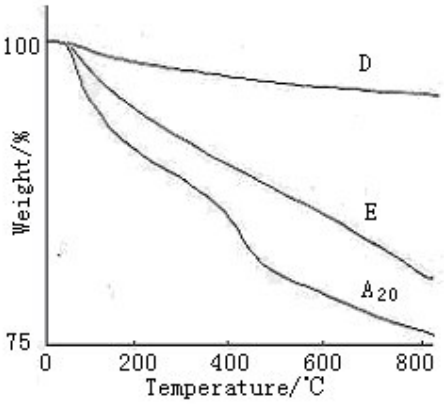

Figure 3. TGA of samples.

Effect of the ageing temperature

Figure 4 shows the XRD patterns of samples templated by C_{16}PyCl at various ageing temperature (20-80 ^oC) for 48 h. The figure demonstrates that ageing temperature in a certain temperature range for appropriate time has a significant effect on the formation of well-defined mesostructure. Of these samples, the one aged at 60 ^oC has mesostructures with the largest d-value (d = 10.9 Å), and the d-value of the mesostructures formed at temperatures >60 ^oC decreases to 10.6 Å; these probably indicate that the collapse of the mesostructure is due to a change of the template's self-assembling structure or an enhancing crystallization of TiO_2. In the meantime, it is noticeable that the d-value of sample aged bellow 40 ^oC decreases with increasing temperature (from 10.3 Å to 10.2 Å), whereas that of sample aged above 40 ^oC increases, what is more, anatase crystal appear at 40 ^oC. These results indicate that the ageing temperature at an appropriate temperature is very effective to form a well-defined TiO_2 mesostructure. Figure 5 is the behavior of the DTA curve of samples.

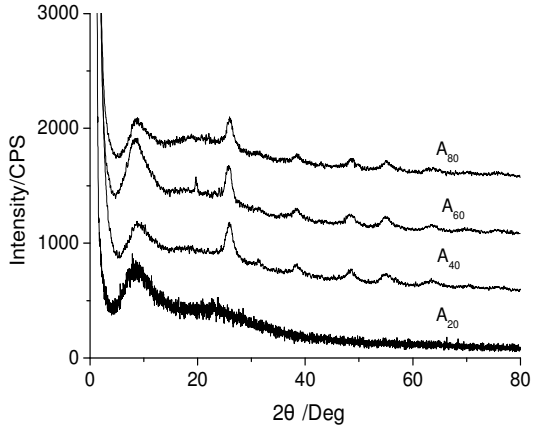

Figure 4. XRD patterns of the samples.

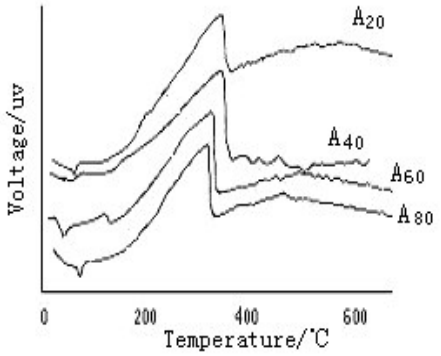

Figure 5. DTA of the samples.

The endothermic peak bellow 100 °C belongs to the desorption of water. There is a big exothermic peak between 360 and 390 °C which corresponds to the larger weight loss produced by surfactants combusting. Moreover, it is found that the decomposition temperature initially increases with the increase of the ageing temperature, then decreases. The decomposition temperature of samples aged at 20, 40, 60 and 80 °C are 375.2, 387.2, 364.1 and 362.3 °C, respectively. These results also prove that C_{16}PyCl can be removed from the synthesized samples by the calcinations above 400 °C.

Effect of the variation of solvents

Figure 6 shows the XRD patterns of samples obtained by different solvents. Samples A_{20}, B and C use C_2H_5OH, C_4H_9OH and $CHCl_3$ as solvents, respectively. Excluding sample B, both sample A and C exhibit low angle reflections of mesoporous materials at $2\theta<10°$, and sample C also demonstrates ordinary crystalline phase of the surfactant. For sample B, it shows only one peak around $2\theta = 38°$ which can be indexed to a lattice with d (004) spacing of 2.62 Å related with anatase. From these images, it can be concluded that the variation of solvents can influence the mesostructure of materials significantly.

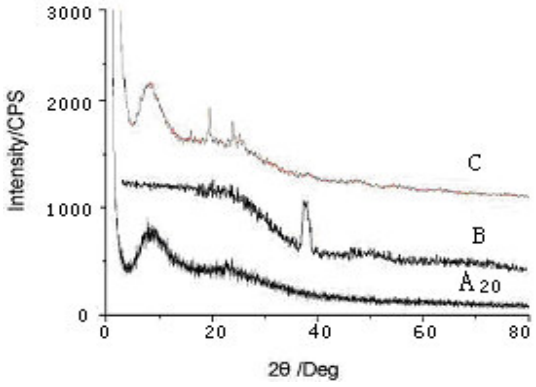

Figure 6. XRD patterns of the samples.

From Table 2, the BET surface areas and pore volume of samples A_{20}, B and C are 310.3, 81.5, 247.9 m^2g^{-1} and 0.7968, 0.2909, 0.5528 cm^3g^{-1}, respectively. Under the present experimental conditions, C_2H_5OH is the best solvent, the results of XRD are in accordance with those of the BET surface areas and pore volume. Figure 7 shows the thermogravimetric analysis curves of samples A_{20}, B, C, which indicates the strong interactions of the associated template with titanium groups. The weight loss of samples A_{20}, B and C are a little different. That is to say, the link of template with Ti species is related to solvents.

Table 2. The textural properties of m-TiO_2.

Samples	A_{20}	A_{40}	A_{60}	A_{80}	A(acid)	A(base)	B	C	D	E
BET surface area(m^2g^{-1})*	310.3	180.1	92.19	129.8	99.49	4.610	81.50	247.9	262.5	292.3
Average pore size (nm)	6.950	7.130	2.950	3.840	6.480	--	7.320	3.710	4.850	4.050
Pore volume (cm^3g^{-1})	0.7968	0.6418	0.1360	0.2490	0.3224	--	0.2909	0.5528	0.6369	0.5920

*Surface area was measured before reaction.

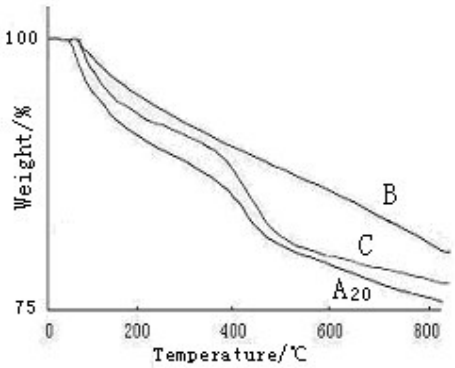

Figure 7. TGA of samples.

Effects of pH

Figure 8 shows the XRD patterns of samples prepared in precursor solutions with the different pH value. The pH value of samples A_{20}, A(acid) and A(base) is 7-8, 3-4 and 9-10, respectively. The small angle diffraction peak ($2\theta<10°$), indicating the formation of a mesostructure, can be seen from only the sample A_{20} from the solutions with pH = 7-8, and this pH range has been considered to be suitable to form mesostructures because of the high stability of Ti species in alkoxide solutions. The data of Figure 8 demonstrate that the optimum pH value of the precursor solution for synthesizing mesostructure TiO_2 seems to exist in the range of 7-8 when C_{16}PyCl is used as template, and the acidic condition is favorable to form the anatase. That is, control of the pH value is necessary to form the large pore TiO_2 mesostructure with C_{16}PyCl template due to induced hydrogen bonding interaction between cationic surfactant and Ti species [17]. It is obvious that easy-operating neutral condition can form mesostructure not only for a restriction on the hydrolysis and condensation process of Ti-alkoxide in the precursor solutions used, but also for an induction of the charge matching between C_{16}PyCl and Ti.

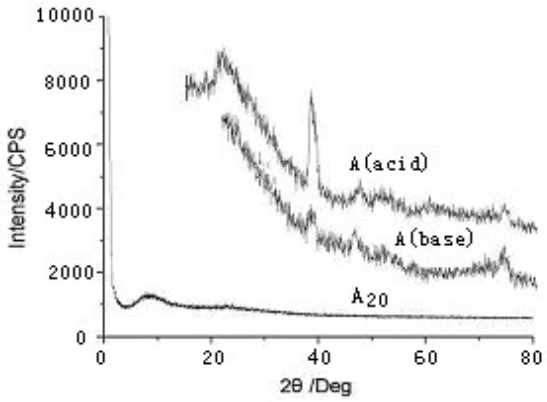

Figure 8. XRD patterns of the samples.

Effect of C_{16}PyCl to TTIP ratio

The results of different molar ratio of C_{16}PyCl to TTIP are summarized in Table 3. It has been found that the molar ratio of C_{16}PyCl to TTIP significantly affects the mesostructure of TiO_2. Figure 9 shows XRD patterns of samples with different C_{16}PyCl/TTIP molar ratios. It is apparent that the d-spacing of mesostructure TiO_2, and the intensity of the peak as well, increases with increasing molar ratio of C_{16}PyCl. In other words, the mesostructure with a better and longer range arrangement is formed with increasing molar ratio of the template. No more increase of the d-spacing is observed for C_{16}PyCl/TTIP molar ratios above 2, and then the intensity of the peak decreases. The results of BET surface areas (see Table 3) show that surface areas increase with increasing molar ratio of C_{16}PyCl/TTIP initially. When the C_{16}PyCl/TTIP molar ratio is 2, the BET surface areas get to the largest (310.3 m^2g^{-1}). Above 2, the BET surface areas decrease with the increase of the C_{16}PyCl/TTIP molar ratio. In addition, average pore size and pore volume have also variety regulation with one accord.

Table 3. Effect of the C_{16}PyCl to TTIP molar ratio.

Sample	C_{16}PyCl to TTIP molar ratio	BET surface area (m^2g^{-1})*	Average pore size (nm)	Pore volume (cm^3g^{-1})
$A_{0.5/1}$	0.5:1	205.7	10.21	1.050
$A_{1.0/1}$	1.0:1	206.5	6.920	0.7140
$A_{2.0/1}$	2.0:1	310.3	6.950	0.7968
$A_{2.5/1}$	2.5:1	304.9	2.330	0.3555
$A_{3.0/1}$	3.0:1	231.6	3.310	0.3833

*Surface area was measured before reaction.

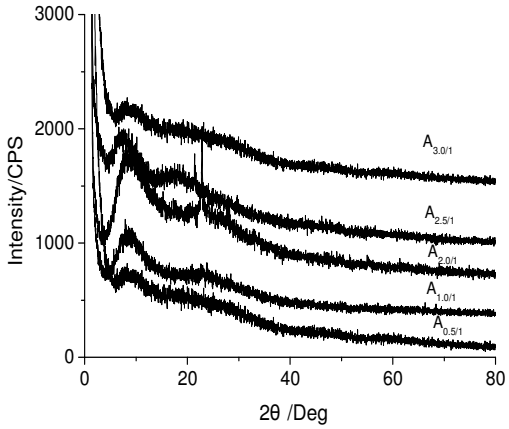

Figure 9. XRD patterns of the samples.

Effect of heat treatment condition

The results of sample A_{20} calcined at different temperature for 3 h are shown in Figure 10. From the XRD patterns, with the increase of calcining temperature, the intensity of low angle diffraction peak decreases, while the d-spacing varies a little. Before being calcined, sample A_{20} has larger pore volume (0.7968 cm^3g^{-1}) and surface areas (310.3 m^2g^{-1}), while they reduce to 0.2987 cm^3g^{-1} and 215.6 m^2g^{-1} at 400 ^oC, respectively. The XRD results show that the mesostructure collapses partly at 400 ^oC. With a rise in calcination temperature to 600 ^oC, the surface areas decrease to 207.1 m^2g^{-1}, but it is large enough in comparison with commodity TiO_2 (1.1 m^2g^{-1}), and the pore volume reduce to 0.1905 cm^3g^{-1}. The XRD results show that the low angle diffraction peak still retaine, only the mesostructure collapses farther partly at 600 ^oC.

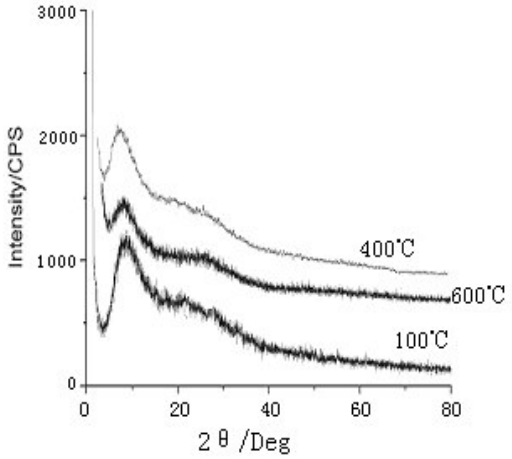

Figure 10. XRD patterns of the samples heated at different temperature for 3 h.

Methanol decomposition

Methanol decomposition to carbon monoxide and hydrogen has recently attracted a growing interest because the endothermic reaction is applicable for waste heat recovery from industries [18]. Palladium is active to the reaction especially when the support is zirconium oxide and cerium oxide on which palladium is highly dispersed [12, 19 -21]. Titanium oxide seems to be an active support, but the dispersion of palladium on the surface is not as high as on zirconium oxide and cerium oxide [12]. Mesoporous materials, on the other hand are also of great interest. In addition to their extensive applications in optics, or ceramics, these materials are also used as catalysts and catalyst supports. The use of high surface area mesoporous oxide supports may give rise to well dispersed and stable metal particles on the surface upon calcination and reduction and thus strongly influence the catalytic performances. Methanol is selectively decomposed to carbon monoxide and hydrogen over the series of ruthenium catalysts. No product such as methane is detected under the reaction conditions. The catalytic activity results of Ru/m-TiO_2 synthesized by easy-operating method for methanol decomposition are given in Figure 11. The activity curves of all catalysts have the similar variation rule, that is, below 260 ^oC, the activity increases with the increase of reaction temperature, whereas the activity reduces slowly above 260 ^oC, which might be due to the formation of a fraction of TiO_x after being reduced using H_2. Then at high temperature, ruthenium particles are mantled partly or space blockage is formed around ruthenium particles because TiO_x species are easily migrated [22]. Comparing to mesoporous 1% Ru/A_{20} and 1% Ru/D, the activity of the catalysts decreases in the following order: 1% Ru/A_{20} > 1% Ru/D. This result was consistent with the order of the BET surface areas at 400 ^oC for 2 h (two of them are 174.3 and 139.1 m^2g^{-1}, respectively). It is concluded that mesoporous material with high surface areas helps to generate the very small ruthenium particles with better distributions, dispersion and stability on the surface of the mesoporous oxide supports. From the curves in Figure 11b, the effect of solvents on the activity is contrary to the order of surface areas of samples. After being calcined at 400 ^oC for 2 h, the BET surface areas of 1% Ru/A_{20} and 1% Ru/C catalysts are 174.3 and 225.9 m^2g^{-1}, respectively. It is concluded that the catalytic activity is not completely depended on dispersion of active components. It may be due to the strong interaction between Ru and TiO_x in 1% Ru/A_{20}, which leads to improve the ability of adsorption hydrogen, so the activity increases [23]. As shown in Figure 11c, the effect of pH on catalytic activity was investigated. The results indicate that the BET surface areas of 1% Ru/A(acid) (pH = 3-4), 1% Ru/A_{20} (pH = 7-8), 1% Ru/A(base) (pH = 9-10) calcined at 400 ^oC for 2 h are similar (173.0, 174.3 and 170.0 m^2g^{-1}, respectively). However, the differences in activity is clearly observed, particularly 1% Ru/A(acid). This can be explained by the different crystal structure of supports, which lead to different strong interaction between ruthenium nanoparticles and oxide species, which may reduce the activation energy of the rate determining step in the methanol decomposition, i.e., decomposition of the surface methoxyl group into surface carbon monoxide and hydrogen [24]. According to these results, it is concluded that the surface area is not the only factor correlated with catalytic activity.

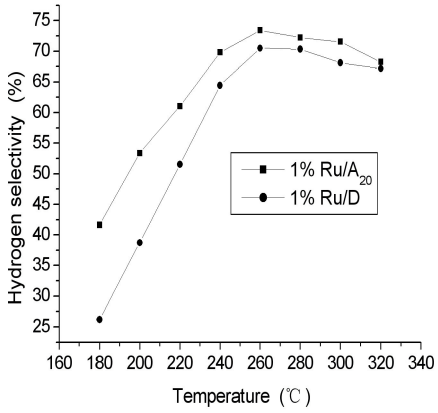

a: Supports prepared by different templates

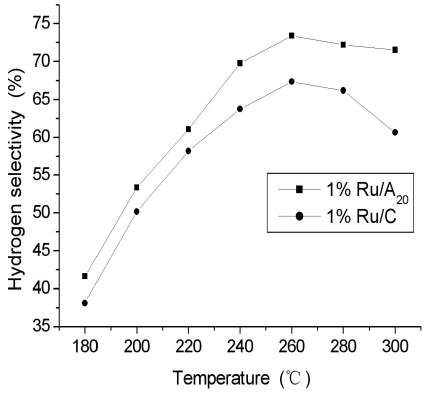

b: Supports prepared in different solvents

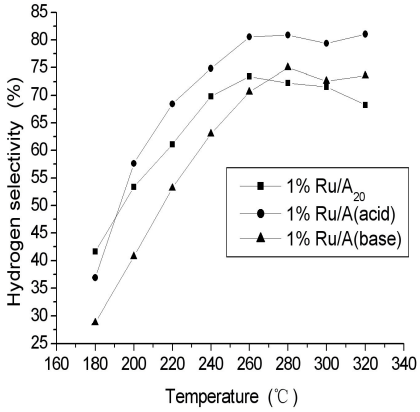

c: Supports prepared at different pH

Figure 11. Relationship between the reaction temperature and the catalytic activity.

ACKNOWLEDGEMENT

The work described above was fully supported by a grant from the Nanchang University, China.

REFERENCES

1. Koh, C.A.; Nooney, R.; Tahir, S. *Catal. Lett.* **1997**, 47, 199.
2. Matthews, L.R.; Avnir, D.; Modestov, A.D.; Smpath, S.; Lev, O. *J. Sol-Gel Sci. Technol*. **1997**, 8, 619.
3. O'Regan, B.; Graetzel, M. *Nature* **1991**, 353, 737.
4. Antonelli, D.M. *Micropor. Mesopor. Mater.* **1999**, 30, 315.
5. Antonelli, D.M.; Ying, J.Y. *Angew. Chem. Int. Ed. Engl.* **1995**, 34, 2014.
6. Dai, Q.; Zhang, Z.; He, N.; Li, P.; Yuan, C. *Mater. Sci. Eng. C* **1999**, 8-9, 417.
7. Nishimura, T.; Omata, T.; Ogisu, Y. *Eco-Energy City System*, Energy Conservation Center: Tokyo; **1999**; p 186.
8. Matsumura, Y.; Kuraoka, K.; Usami, Y.; Yazawa,T.; Haruta, M. *Catal. Today* **1998**, 45, 191.
9. Wickham, D.T.; Logsdon, B.W.; Cowley, S.W.; Butler, C.D. *J. Catal.* **1991**, 128, 198.
10. Shiozaki, R.; Hayakawa, T.; Liu, Y.; Ishii, T.; Kumagai, M.; Hamakawa, S.; Suzuki, K.; Itoh, T.; Shishido, T.; Takehira, K. *Catal. Lett.* **1999**, 58, 131.
11. Fan, L.; Fujimoto, K. *J. Catal.* **1994**, 150, 217.
12. Usami, Y.; Kagawa, K.; Kawazoe, M.; Matsumura, Y.; Sakurai, H.; Haruta, M. *Appl. Catal.* **1998**, 171, 123.
13. Matsumura, Y.; Kuraoka, K.; Yazawa, T.; Haruta, M. *Catal. Today* **1998**, 45, 191.
14. Yang, P.Y.; Zhao, D.Y.; Margolese, D.I.; Chmelka, B.F.; Stucky, G.D. *Nature* **1998**, 396, 152.
15. Zhao, X.S.; Wang, Q.X.; Xu, L.Y.; Xie, S.J. *Chinese J Catalysis* **1995**, 5, 415.
16. Abe, T.; Taguchi, A.; Jwamoto, M. *Chem. Mater.* **1995**, 7, 1429.
17. Zhao, D.; Huo, Q.; Feng, J.; Chmelka, B.F.; Stucky, G.D. *J. Am. Chem. Soc.* **1998**, 120, 6024.
18. Panel on new Directions in Catalytic Science and Technology, Board on Chemical Sciences and Technology, National Research Council, *Catalysis Look to the Future*, National Academy Press: Washington, DC; **1992**.
19. Usami, Y.; Kagawa, K.; Kawazoe, M.; Matsumura, Y.; Sakurai, H.; Haruta, M. *Stud. Surf. Sci. Catal.* **1998**, 118, 83.
20. Matsumura, Y.; Ichihashi, Y.; Morisawa, Y.; Okumura, M.; Haruta, M. *Stud. Surf. Sci. Catal.* **2000**, 130, 2315.
21. Shen, W.J.; Matsumura, Y. *Phys. Chem. Chem. Phys.* **2000**, 2, 1519.
22. Haller, G.L.; Resasco, D.E. *Adv. Catal.* **1990**, 37, 1.
23. Yang, C.; Ren, J.; Sun, Y.H. *J. Fuel Chem. Tech. (China)* **2001**, 8, 157.
24. Tokunaga, O.; Satoh, Y.; Fukushima, T.; Ogasawara, S. *Sekiyu Gakkaishi* **1990**, 33, 173.